

CAROTID ARTERY WALL SEGMENTATION IN ULTRASOUND IMAGE SEQUENCES USING A DEEP CONVOLUTIONAL NEURAL NETWORK

Nolann Lainé^{*} Guillaume Zahnd[†] Hervé Liebgott^{*} Maciej Orkisz^{*}

^{*} Univ Lyon, INSA-Lyon, Université Lyon 1, UJM-Saint Etienne, CNRS, Inserm, CREATIS UMR 5220, U1206, F-69621, Lyon, France

[†] Institute of Biological and Medical Imaging, Helmholtz Zentrum München, Neuherberg, Germany

ABSTRACT

The objective of this study is the segmentation of the intima-media complex of the common carotid artery, on longitudinal ultrasound images, to measure its thickness. We propose a fully automatic region-based segmentation method, involving a supervised deep-learning approach based on a dilated U-net network. It was trained and evaluated using a 5-fold cross-validation on a multicenter database composed of 2176 images annotated by two experts. The resulting mean absolute difference ($< 120 \mu\text{m}$) compared to reference annotations was less than the inter-observer variability ($\approx 180 \mu\text{m}$). With a 98.7% success rate, *i.e.*, only 1.3% cases requiring manual correction, the proposed method has been shown to be robust and thus may be recommended for use in clinical practice.

Index Terms— Atherosclerosis, carotid artery, segmentation, ultrasound, deep learning, U-net, dilated convolution.

1. INTRODUCTION

According to the World Health Organisation, cardiovascular diseases (CVDs), particularly atherosclerosis, are considered the leading cause of death worldwide [1] although they are preventable [2]. Prevention requires screening by means of a non-ionising and inexpensive imaging modality. Ultrasound (US) imaging has these characteristics and is routinely used to explore the common carotid artery (CCA), which is often considered as the sentinel of atherosclerosis [3]. An early sign of this disease onset is the arterial wall thickening. To measure the thickness of interest, the contours of the intima-media complex (IMC), namely, lumen-intima (LI) and media-adventitia (MA) interfaces, need to be identified (Fig. 1).

The majority of methods in the literature use contour-based approaches [4, 5, 6, 7] to exploit the intensity peaks caused by the echoes at the interfaces, named double-line pattern. Region-based approaches are less used and combine despeckling with threshold-based segmentation [8, 9].

Recently, deep-learning (DL) has been successfully used in vascular US-image segmentation to enhance the structures of interest prior to the actual delineation by more conventional contour-based methods [10, 11, 12]. The drawback of

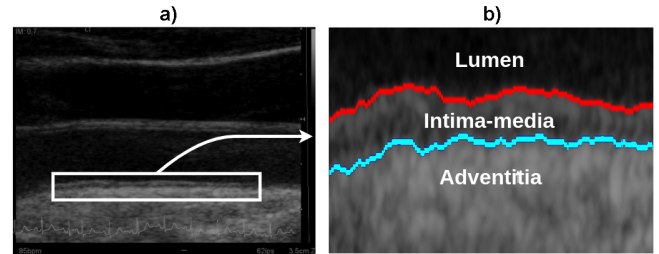


Fig. 1. Example of *IMC* segmentation by the proposed method: *a)* Longitudinal view of the CCA in a B-mode ultrasound image. *b)* Enlarged region detailing the intima-media complex with its interfaces, LI (red) and MA (cyan).

these approaches is the necessity to combine a learnable pre-processing operation with an analytic segmentation task.

The main contribution of the present work is a supervised learnable segmentation method, designed to extract the two contours of the *IMC* in B-mode *US* images. Anatomical interfaces, in asymptomatic arteries without plaque, are localized by a region-based approach using a collection of overlapping patches. The proposed patch-based solution successfully addresses the challenge of segmenting with a unique network architecture the entire exploitable part of the *IMC* despite strong variations in its width from one image to another.

2. DATA AND METHOD

All training and evaluation processes were carried out on a publicly available multi-center database (<http://dx.doi.org/10.17632/epv535fss7.1>). Images were acquired from both sides of the neck, for a total of 2176 images. Refer to [13] for more details.

For this study, we considered two experts (*A1* and *A2*) who independently selected a region of interest (*ROI*), where interfaces were perceptible, and traced control points within it. To obtain smooth contours piecewise cubic Hermite interpolating polynomial (*PCHIP*) was applied using *MATLAB*, Version 2020b (The Math Works, Inc.).

The proposed solution builds on a convolutional neural

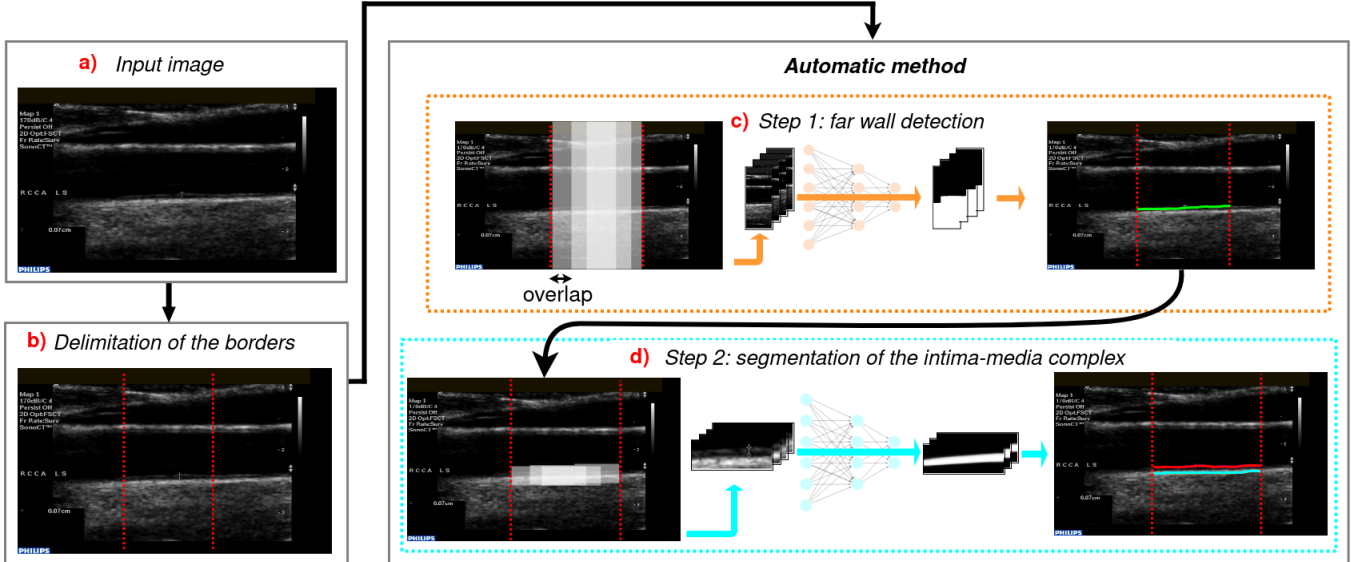


Fig. 2. Flowchart of the proposed method. *a*) Input image. *b*) User delimitation of the left and right borders of the ROI. *c*) Far wall detection: patches are extracted through a sliding window with overlap within ROI borders; post-processing of predicted overlapping masks leads to extraction of the median axis (green). *d*) IMC segmentation: overlapping patches are picked along the median axis and post-processing of the predicted masks leads to extraction of the LI (red) and MA (cyan) interfaces.

network known as U-net [14], with dilated convolutions on the bottleneck to increase its receptive field [15]. As the annotations are available for ROIs of variable width, we cut the ROI into fixed-size horizontally overlapping patches, and it is also a way to apply the same receptive field on each image with a control pixel size. A post-processing combines the predictions made within the patches to extract smooth contours over the entire ROI regardless of its width. The core of the method consists of two steps: approximately detecting the far wall (Fig. 2c), and precisely segmenting the IMC contours (Fig. 2d).

Code is available at <https://github.com/n13769/caroSegDeep>.

2.1. Detection of the far wall

Like in many state-of-the-art methods [6, 9, 10, 11], the far wall is first detected and is considered as the initialization step. Here, the patches are of full image height and 128-pixel width, and the corresponding U-net will be referred to as Θ_{FW} . We first describe the pre-processing and the training phase, then we specify the post-processing chosen to obtain the curve approximately localizing the far wall on the entire ROI width from patch-wise predictions inferred using Θ_{FW} .

Pre-processing and training: All images of the database were resampled to a constant height of 512 pixels (as the native height of all images in the database is around 600 pixels, the distortion thus introduced was minimal). For training

data, the median axis of the IMC was defined as the line halfway between LI and MA annotations, interpolated across the entire width of the ROI, and a reference mask (M_{ROI}) was generated by setting all pixels below the median axis to 1 and the others to 0. Then ROI and M_{ROI} were identically cut into patches and a 100-pixel overlap between patches aimed at data augmentation. Thus obtained patches with their associated masks (Fig. 3) were fed into the training process, which used the ADAM optimizer and a loss function experimentally chosen to minimize the Hausdorff distance and maximize the overlay with respect to the reference masks, namely, the sum of the binary cross-entropy and the Dice loss.

Inference and post-processing: Prior to inference, each image is resampled as described above, and then the corresponding ROI is cut into 128×512 -pixel patches. Next, all patches are segmented using Θ_{FW} . Knowing the location and the size of each patch, two maps are created:

- **prediction map:** contains, for each pixel, the sum of values predicted by Θ_{FW} .
- **overlay map:** contains, for each pixel, the number of overlapping patches it belonged to.

Dividing the prediction map by the overlay map provides, for each pixel, an average value in the range $[0, 1]$, which is then binarized by using a threshold of 0.5, to obtain the segmentation map. The latter is cleaned by retaining the largest connected component. The median axis we seek is the upper boundary of thus segmented region. Eventually, a third order polynomial regression is applied to the retrieved boundary

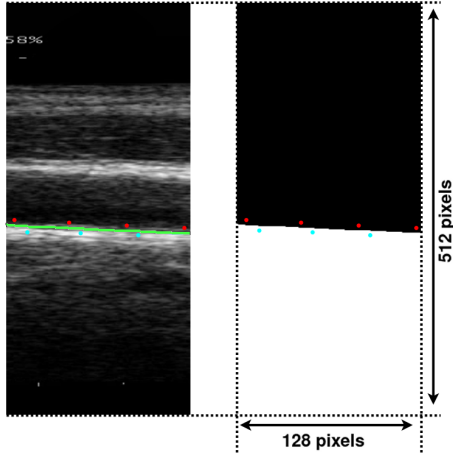


Fig. 3. Data used during the far wall detection training phase. Red and cyan dots represent the annotations for *LI* and *MA* interfaces, respectively. The green curve is the median axis calculated from the interpolated annotations.

with the aim of increasing the robustness of the method.

2.2. Segmentation of the IMC

The far wall approximation is used to initialize the actual segmentation of the *IMC*, which uses many similar concepts explained in Section 2.1: overlapping patches of 128×512 pixels, an overlay map, a prediction map, a similar post-processing except that two contours are extracted (the *LI* and *MA* interfaces), as well as the same optimizer, loss function, and U-net architecture. The dilated U-net trained here will be referred to as Θ_{IMC} . Hereafter, we emphasize the specific choices made for this step.

Pre-processing and training: The segmentation task has to be as accurate as possible, hence the algorithm works at a sub-pixel resolution. To this purpose, the vertical pixel size of the images was homogenized to $5 \mu\text{m}$ using a linear interpolation. According to this physical size, the patch height of 512 pixels roughly corresponds 2.6 mm, which aims to encompass the *IMC*, knowing that the average *IMC* thickness is about 0.8 mm. For training, the ground truth was then deduced from thus interpolated images (Fig. 4): each pixel located between the annotated *LI* and *MA* interfaces was set to 1, and the others to 0. Unlike the far wall detection, the patches were extracted along the median axis: at each abscissa x_i , the mean ordinate y_i of the median axis was computed on the patch width and three patches were extracted, respectively centered at y_i , $y_i + 128$, and $y_i - 128$. This data augmentation attempted to cope with possibly inaccurate far-wall approximation as well as with tilted arteries.

Inference and post-processing: During inference, the

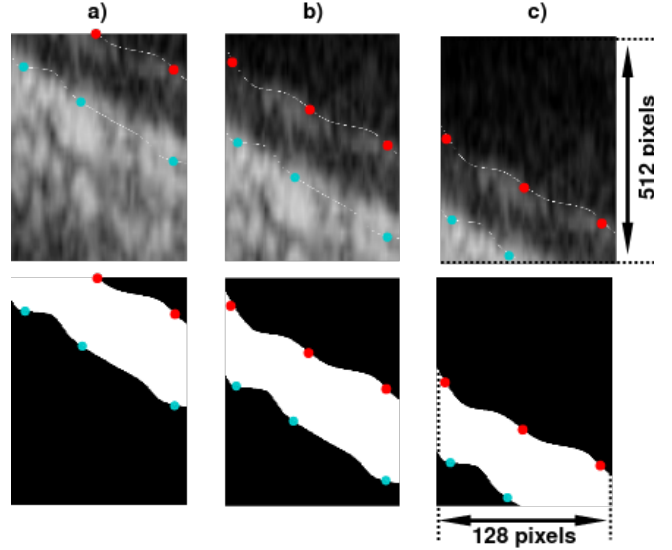


Fig. 4. Data used during the training phase for *IMC* segmentation. Patches and their associated masks located at: *a*) $(x_i, y_i - 128)$, *b*) (x_i, y_i) , and *c*) $(x_i, y_i + 128)$. Red and cyan dots represent the corresponding annotations for *LI* and *MA* interfaces, respectively. The dashed curves were obtained by interpolating the annotations.

patches are extracted along the far-wall approximation resulting from the first step (Section 2.1). At each abscissa x_i three or more patches are captured at different ordinates, depending on the tilt of the median axis. The predictions made by Θ_{IMC} in all patches are combined into a prediction map, and then the segmentation map is derived thereof, as described above. Finally, the *LI* and *MA* interfaces are respectively defined as the upper and lower boundaries of thus segmented region.

3. RESULTS

The evaluation was carried out using 5-fold cross-validation, so as to assess each network on data not seen during its training. In each fold, the database was split into training (60%), validation (20%), and testing (20%) subsets. Thus, five pairs of networks Θ_{FW} and Θ_{IMC} were trained and tested independently, and the results reported here are the merging of the test sets of these five pairs, thus evaluating the method on the entire database.

In the proposed cascade approach, a failure of the first step (far wall detection) will trigger a failure of the second step (*IMC* segmentation). To conduct a fair evaluation of both steps, we first quantified the success rate of the first step alone, then we quantified the accuracy of the second step by manually enforcing valid initial conditions when needed.

Robustness of the far wall detection: After visual inspection, 36 predicted median axes (1.3% of the database) were considered as failures, *i.e.* curves unusable to initialize the *IMC* segmentation step. Hence, the success rate was of 98.7% and in the 36 images with failures, the median axis was manually redrawn using a home-made graphical interface.

Accuracy of the *IMC* segmentation: The segmentation error was quantified by measuring the column-wise median absolute difference (*MAD*) between the method output and the annotations performed by *AI*, for *LI*, *MA*, and *IMT*. These results are summarized in Table 1.

Table 1. Mean absolute difference (\pm standard deviation) of segmentation results, for contour locations (*LI*, *MA*) and thickness quantification (*IMT*). Middle column: Method against reference annotations. Right column: Inter-observer variability.

Measure	Method vs. <i>AI</i> (μm)	<i>A2</i> vs. <i>AI</i> (μm)
LI	119 \pm 124	183 \pm 160
MA	107 \pm 120	177 \pm 149
IMT	161 \pm 159	254 \pm 211

4. DISCUSSION AND CONCLUSION

We developed and assessed an almost-automatic (two user mouse clicks to define the limits of the exploitable *ROI*) deep-learning method to extract the contours of the intima-media complex in longitudinal B-mode ultrasound images of the carotid artery. The method first approximately localizes the far wall, and then segments the anatomical interfaces of interest. The proposed approach allows segmenting *ROIs* of variable width without having to resize the images.

Robustness of the far-wall localization step is a prerequisite for overall correct segmentation. This step was successful in all but 1.3% of the images, showing the robustness of the method. The actual segmentation step achieved good accuracy, with errors smaller than the inter-observer variability, both in terms of mean absolute difference in contour location (less than 120 μm vs. \sim 180 μm) and of standard deviation (\sim 120 μm vs. \sim 150 μm). These results were comparable with the best-performing state-of-the-art methods evaluated on the same database [13]. Based on supervised learning, our method has the potential to increase its performance by using larger and more diverse database for training, which was proved in a recent study, where our method outperformed the existing ones [16].

The largest errors occurred in the presence of calcified plaques. As the work presented here was oriented towards asymptomatic plaque-free subjects, images with plaques were not expected. Nevertheless, we anticipate that results might be improved by enriching the database with such images appropriately annotated, and subsequently re-training the net-

works. This avenue deserves investigation.

In conclusion, with a 98.7% success rate and the accuracy comparable to human experts, the proposed method may be recommended for use in clinical practice.

5. ACKNOWLEDGMENTS

This work was partly supported, via NL’s doctoral grant, by the LABEX PRIMES (ANR-11-LABX-0063) of Université de Lyon, within the program “Investissements d’Avenir” (ANR-11-IDEX-0007) operated by the French National Research Agency (ANR).

The authors have no relevant financial or non-financial interests to disclose.

6. COMPLIANCE WITH ETHICAL STANDARDS INFORMATION

The data from human subjects used in this work were obtained and treated in line with the principles of the Declaration of Helsinki. Approval was granted by the Ethics Committees of the institutions involved in creating the multicentric database, from which these data were accessed.

7. REFERENCES

- [1] S Kaptoge, L Pennells, D De Bacquer, MT Cooney, M Kavousi, G Stevens, et al., “World health organization cardiovascular disease risk charts: revised models to estimate risk in 21 global regions,” *Lancet Glob Health*, vol. 7, no. 10, pp. e1332–e1345, 2019.
- [2] HC McGill Jr, CA McMahan, and SS Gidding, “Preventing heart disease in the 21st century: implications of the pathobiological determinants of atherosclerosis in youth (PDAY) study,” *Circulation*, vol. 117, no. 9, pp. 1216–1227, 2008.
- [3] F Yousefi Rizi, J Au, H Yli-Ollila, S Golemati, M Makūnaitė, M Orkisz, et al., “Carotid wall longitudinal motion in ultrasound imaging: An expert consensus review,” *Ultrasound Med Biol*, vol. 46, no. 10, pp. 2605–2624, October 2020.
- [4] S Delsanto, F Molinari, P Giustetto, W Liboni, S Badalamenti, and JS Suri, “Characterization of a completely user-independent algorithm for carotid artery segmentation in 2-D ultrasound images,” *IEEE Trans Instrum Meas*, vol. 56, no. 4, pp. 1265–1274, 2007.
- [5] CP Loizou, CS Pattichis, M Pantziaris, T Tyllis, and A Nicolaides, “Snakes based segmentation of the common carotid artery intima media,” *Med Biol Eng Comput*, vol. 45, no. 1, pp. 35–49, 2007.

- [6] G Zahnd, K Kapellas, M Van Hattem, A Van Dijk, A Sérusclat, P Moulin, et al., “A fully-automatic method to segment the carotid artery layers in ultrasound imaging: Application to quantify the compression-decompression pattern of the intima-media complex during the cardiac cycle,” *Ultrasound Med Biol*, vol. 43, no. 1, pp. 239–257, 2017.
- [7] KV Raj, J Joseph, PM Nabeel, and M Sivaprakasam, “Automated measurement of compression-decompression in arterial diameter and wall thickness by image-free ultrasound,” *Comput Methods Programs Biomed*, vol. 194, pp. 105557, 2020.
- [8] Y Nagaraj, P Madipalli, J Rajan, PK Kumar, and AV Narasimhadhan, “Segmentation of intima media complex from carotid ultrasound images using wind driven optimization technique,” *Biomed Signal Process Control*, vol. 40, pp. 462–472, 2018.
- [9] K Wang, Y Pu, Y Zhang, and P Wang, “Fully automatic measurement of intima-media thickness in ultrasound images of the common carotid artery based on improved Otsu’s method and adaptive wind driven optimization,” *Ultrason Imaging*, vol. 42, no. 6, pp. 245–260, 2020.
- [10] R-M Menchón-Lara, J-L Sancho-Gómez, and A Bueno-Crespo, “Early-stage atherosclerosis detection using deep learning over carotid ultrasound images,” *Appl Soft Comput*, vol. 49, pp. 616–628, 2016.
- [11] C Qian, E Su, and X Yang, “Segmentation of the common carotid intima-media complex in ultrasound images using 2-D continuous max-flow and stacked sparse auto-encoder,” *Ultrasound Med Biol*, vol. 46, no. 11, pp. 3104–3124, 2020.
- [12] J Shin, N Tajbakhsh, RT Hurst, CB Kendall, and J Liang, “Automating carotid intima-media thickness video interpretation with convolutional neural networks,” in *Proc IEEE Conf Computer Vision Pattern Recogn*, 2016, pp. 2526–2535.
- [13] K Meiburger, G Zahnd, F Fajta, C P Loizou, C Carvalho, D A Steinman, L Gibello, R M B, F Marzola, R Clarenbach, et al., “Carotid ultrasound boundary study (CUBS): An open multicenter analysis of computerized intima-media thickness measurement systems and their clinical impact,” *Ultrasound in Medicine & Biology*, vol. 47, no. 8, pp. 2442–2445, 2021.
- [14] O Ronneberger, P Fischer, and T Brox, “U-net: Convolutional networks for biomedical image segmentation,” in *Int Conf Med Image Computing and Computer-assisted Intervention – MICCAI*, 2015, pp. 234–241.
- [15] NH Meshram, CC Mitchell, S Wilbrand, RJ Dempsey, and T Varghese, “Deep learning for carotid plaque segmentation using a dilated U-net architecture,” *Ultrason Imaging*, vol. 42, no. 4-5, pp. 221–230, 2020.
- [16] K Meiburger, F Marzola, G Zahnd, F Fajta, C P Loizou, N Lainé, C Carvalho, D A Steinman, L Gibello, R M Bruno, et al., “Carotid ultrasound boundary study (CUBS): Technical considerations on an open multi-center analysis of computerized measurement systems for intima-media thickness measurement,” *Computers in Biology & Medicine*, 2022.